BMC Veterinary Research

RESEARCH

Open Access

Anti-tumor effects of rivoceranib against canine melanoma and mammary gland tumour in vitro and in vivo mouse xenograft models

Qiang Li[1†], You-Seok Kim[2,3†], Ju-Hyun An[2], Jin-Ah Kwon[4], Sang-Hyun Han[4], Woo-Jin Song[5*] and Hwa-Young Youn[2*]

Abstract

Background: Rivoceranib, a novel tyrosine kinase inhibitor, exhibits anti-tumour effects by selectively blocking vascular endothelial growth factor receptor-2 (VEGFR2) in cancer cells. Recently, the therapeutic effects of rivoceranib on solid tumours have been elucidated in human patients. However, the anti-tumour effects of rivoceranib against canine cancer remain unclear. Here, we investigated the anti-tumour effects of rivoceranib using in vitro and in vivo mouse xenograft models.

Methods: We performed cell proliferation, cell cycle, and migration assays to determine the effects of rivoceranib on canine solid tumour cell lines in vitro. Furthermore, apoptosis and angiogenesis in tumour tissues were examined using a TUNEL assay and immunohistochemistry methods with an anti-cluster of differentiation-31 antibody, respectively. Additionally, the expression levels of cyclin-D1 and VEGFR2 activity were determined using western blot analysis.

Results: Rivoceranib treatment showed anti-proliferative effects and mediated cell cycle arrest in the canine melanoma cell line (LMeC) and the mammary gland tumour (MGT) cell line (CHMp). In animal experiments, rivoceranib decreased the average volume of LMeC cells compared to that following control treatment, and similar results were observed in CHMp cells. Histologically, rivoceranib induced apoptosis and exerted an anti-angiogenic effect in tumour tissues. It also downregulated the expression of cyclin-D1 and inhibited VEGFR2 activity.

Conclusion: Our results show that rivoceranib inhibits proliferation and migration of tumour cells. These findings support the potential application of rivoceranib as a novel chemotherapeutic strategy for canine melanoma and MGTs.

Keywords: Dog, Mammary gland tumour, Melanoma, Rivoceranib, VEGFR2

*Correspondence: ssong@jejunu.ac.kr; hyyoun@snu.ac.kr
†Qiang Li and You-Seok Kim contributed equally to this work.
[2] Laboratory of Veterinary Internal Medicine, Department of Veterinary Clinical Science, College of Veterinary Medicine, Seoul National University, Seoul 08826, Republic of Korea
[5] Department of Veterinary Internal Medicine and Research Institute of Veterinary Science, College of Veterinary Medicine, Jeju National University, Jeju 63243, Republic of Korea
Full list of author information is available at the end of the article

Background

Cancer is one of the leading causes of death in dogs, and more than 50% of dogs older than 10 years of age develop at least one malignant tumour [1]. One of the most common malignant tumours in female dogs is the mammary gland tumour (MGT) [2]. In addition, a relatively common cancer in dogs is melanoma, which can occur in the

oral cavity, eye, mucocutaneous junction, nail bed, foot pad, or gastrointestinal tract [3, 4]. Conventional alkylating agents for adjuvant chemotherapy (pulse or metronomic) have been used for MGT or melanoma dogs [5, 6]. Furthermore, recently, recombinant tyrosine kinase inhibitors such as toceranib and masitinib have been prescribed for clinical trials for dogs with solid tumours [1, 7, 8]. However, further clinical studies with large population, and research studies demonstrating their underlying mechanisms are needed.

Angiogenesis has been identified to play a crucial role in solid tumour malignancies and is essential for tumour proliferation, survival, and metastasis [8–10]. The vascular endothelial growth factor (VEGF) family and its receptors (VEGFRs) are considered to comprise the core components in tumour angiogenesis-related molecular mechanisms [11]. Recently, the possibility of inhibiting tumour cell signals arising from the activation of VEGFR2 has been demonstrated through several pharmacodynamic approaches, including receptor blockade (ramucirumab), seizure of the ligand (bevacizumab), and use of small-molecule inhibitors (sorafenib, sunitinib, apatinib, cediranib, and telatinib) [12].

Rivoceranib (also known as apatinib), a novel oral small-molecule selective tyrosine kinase inhibitor of VEGFR2, blocks endothelial and tumour cell proliferation and migration, thus inhibiting tumour growth [13, 14]. Previous studies have demonstrated its improved therapeutic efficacy against various types of carcinoma in humans [15–17]. Furthermore, our group previously reported that rivoceranib showed in vitro anti-tumor activity in canine MGT (CIPp and CIPm; derived from primary site and metastatic lymph node, respectively, with mammary adenocarcinoma) cell lines [18]. However, it is unknown whether rivoceranib plays a similar role in canine melanoma (LMeC; derived from metastatic lymph node with oral mucosa melanoma) and MGT (CHMp; derived from primary site with inflammatory mammary adenocarcinoma) cell lines [19, 20].

In this study, we aimed to investigate the anti-tumour effects of rivoceranib in in vitro and in vivo mouse xenograft models of canine melanoma (LMeC) and MGT (CHMp). The results provide novel insights into the inhibition of VEGFR2 by rivoceranib in canine cancer cells.

Results

Rivoceranib inhibits the proliferation and migration of canine melanoma and MGT cell lines in vitro

To assess the effects of rivoceranib on the proliferation of LMeC and CHMp cells, they were treated with different concentrations of the anti-cancer drug for 24, 48, and 72 h. Results of the cell counting kit (CCK)-8 assay showed that rivoceranib elicited inhibitory effects in a dose-dependent manner in both cell lines (Fig. 1A, B). Cell proliferation was significantly reduced at 25 μM after 24, 48, and 72 h of treatment compared to that in the control groups of both cell lines. Cell proliferation was also significantly reduced following treatment with 6.25 μM (LMeC) and 12.5 μM (CHMp) of rivoceranib after 48 h compared to that in the control group. However, no significant reduction in cell proliferation was observed at 3.125 μM (LMeC) and 12.5 μM (CHMp) of rivoceranib after 72 h. Therefore, for subsequent experiments, we treated the cells with 0, 12.5, and 25 μM of rivoceranib for 48 h.

Rivoceranib promotes cell cycle arrest in canine tumour cell lines in vitro

The effect of rivoceranib on the cell cycle progression of LMeC and CHMp cells was investigated using fluorescence-activated cell sorting (FACS). The cells were treated with different concentrations (0, 12.5, and 25 μM) of rivoceranib for 48 h. These cells were harvested and analysed to determine their distribution among the G0/G1, S, and G2/M phases of the cell cycle. As shown in Fig. 2A, the G0/G1 ratio in the rivoceranib-treated groups was significantly higher than that in the control group (0 μM) in both cell lines, whereas the distribution of cells in the G2/M phase was significantly reduced in both the 12.5-and 25 μM-treated groups compared to that in the untreated control group. In addition, the S phase distribution of LMeC cells was significantly reduced in both the 12.5-and 25 μM-treated groups compared to that in the control group. In contrast, the S phase distributions of CHMp cells were similar in the rivoceranib-treated and untreated control groups.

The proteins extracted from the collected LMeC and CHMp cells were analysed by western blotting. A comparison of relative band intensities confirmed that the expression of cyclin-D1 was significantly lower in the rivoceranib-treated groups than in the untreated control group, and the difference between the 12.5-and 25 μM-treated groups was also significant in both cell lines (Fig. 2B). These results suggest that rivoceranib induces G0/G1 cell cycle arrest through the downregulation of cyclin-D1, thereby inhibiting cell cycle progression in LMeC and CHMp cells.

Rivoceranib inhibits migration and induces apoptosis in canine tumour cell lines in vitro

The effect of rivoceranib on the migration abilities of LMeC and CHMp cells was evaluated using a wound-healing assay. As shown in Fig. 3, migration was significantly reduced in cells treated with rivoceranib in

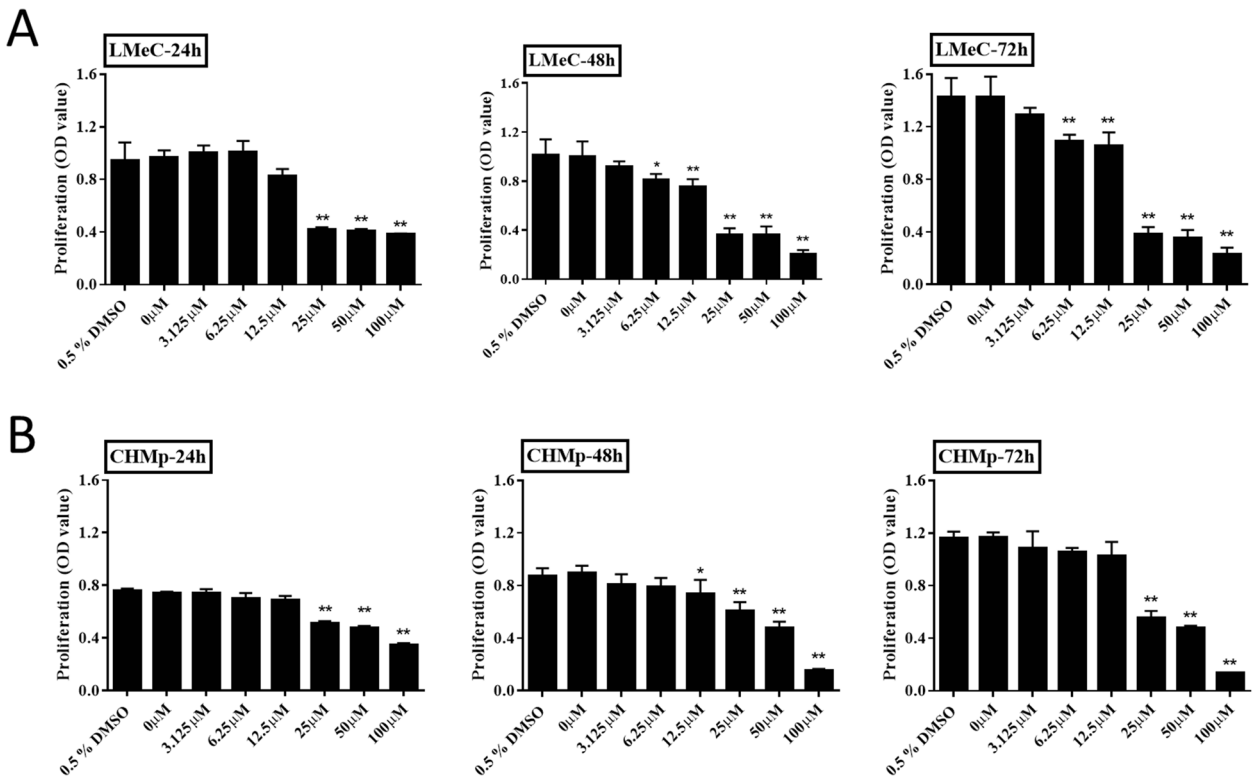

Fig. 1 Effects of rivoceranib on the proliferation of canine solid tumour cell lines in vitro. **A**, **B** Viability of LMeC and CHMp cells after treatment with different concentrations of rivoceranib at 24, 48, and 72 h of treatment. All experiments were performed in triplicate. The data represent the mean ± standard deviation obtained from three independent experiments. * $p < 0.05$, ** $p < 0.01$ versus the control group (0.5% dimethyl sulfoxide) at the same time point

a concentration-dependent manner in both cell lines. These results showed the ability of rivoceranib to inhibit the mobility of canine tumour cell lines in vitro.

To evaluate apoptosis, LMeC and CHMp cells treated with rivoceranib for 48 h were harvested and analysed by FACS after Annexin V/ propidium iodide (PI) dual staining. The percentage of apoptotic cells was significantly increased in the cells treated with 12.5 and 25 μM rivoceranib compared to that in the untreated control group in both cell lines (Fig. 4). These results showed that rivoceranib also induces apoptosis in canine tumour cell lines in vitro.

Rivoceranib suppresses tumour growth in xenograft mouse models

To further determine the anti-tumour activity of rivoceranib in vivo, LMeC and CHMp cell-xenografted mice were orally administered various concentrations of rivoceranib daily. The tumour volume in the control group (vehicle) rapidly increased compared to that in the treated groups. In the LMeC cell line, after 29 days of treatment, the tumour growth curve showed that there was a significant reduction in the tumour volume in the rivoceranib (150 and 300 mg/kg)-treated groups compared to that in the control group (Fig. 5A). In the CHMp cell line, after 16 days of treatment, the 150 and 300 mg/kg rivoceranib-treated groups exhibited a more significant inhibition of tumour volume growth (Fig. 5B) than the control group.

Furthermore, tumour weight was also measured after the mice were sacrificed; the results showed that the tumour weight significantly decreased in the mice treated with rivoceranib in a dose-dependent manner (Fig. 5C) in both cell lines. To detect severe side effects of rivoceranib in mouse models, body weight was also measured. The body weights of mice in the treatment and control groups were similar, with no significant differences observed (Fig. 5D) in both cell lines.

Rivoceranib downregulates VEGFR2 phosphorylation and cyclin-D1 expression in vivo

We further investigated the effects of rivoceranib on VEGFR2 phosphorylation and cyclin-D1 expression. The results revealed that cyclin-D1 expression and

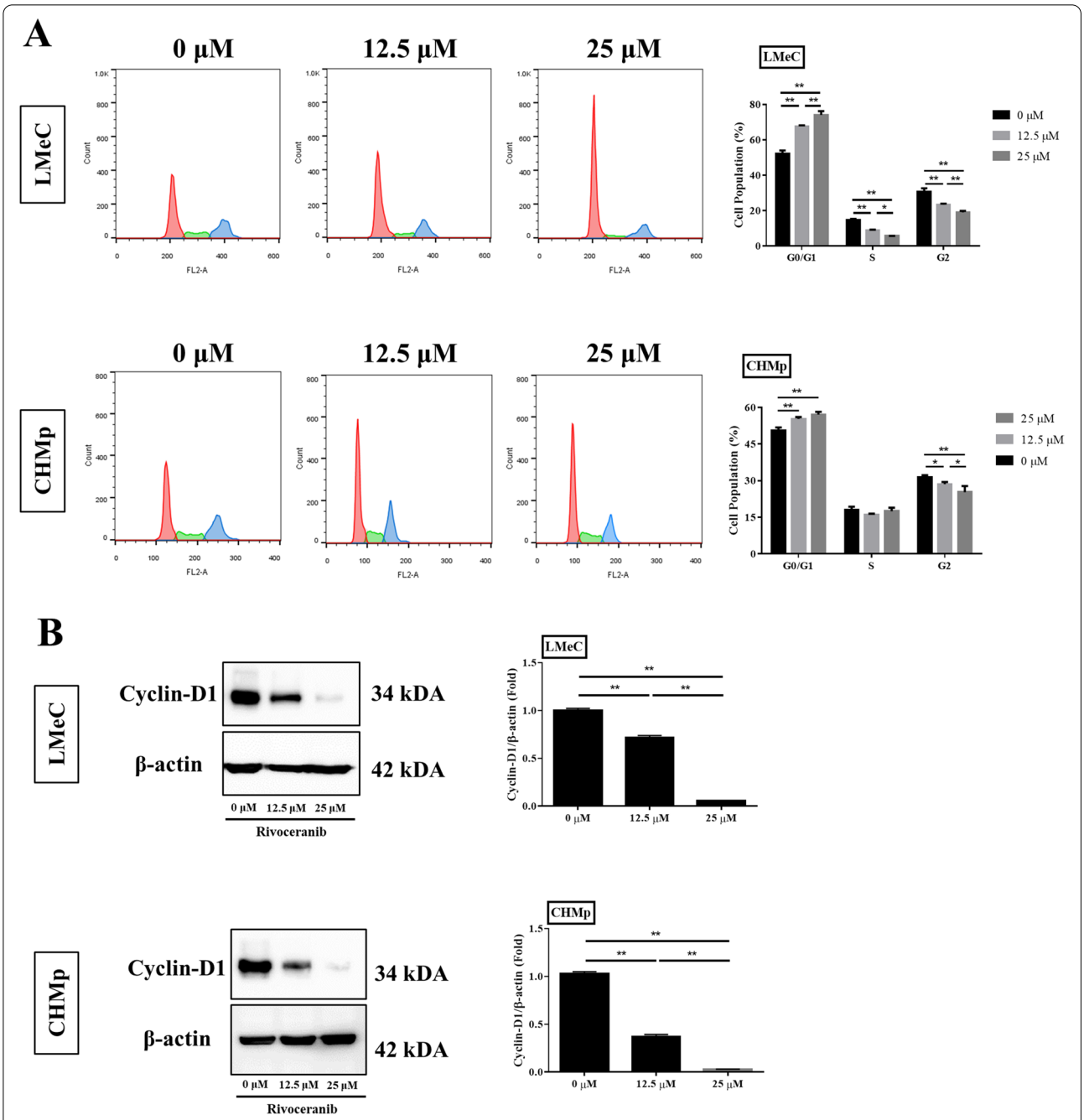

Fig. 2 Effects of rivoceranib on cell cycle arrest in vitro. **A** Cell cycle distribution of LMeC and CHMp cells treated with rivoceranib was analysed by flow cytometry at 48 h. **B** The expression levels of cyclin-D1 were measured using western blot analysis. The intensity of the band on the films is presented as the relative ratio of cyclin-D1 to the band intensity of β-actin. Cropped blots are displayed. Samples were derived from same experiment, and blots were processed in parallel. The data represent the mean ± standard deviation obtained from three independent experiments. * $p < 0.05$, ** $p < 0.01$

VEGFR2 phosphorylation were significantly decreased in the rivoceranib-treated groups in a dose-dependent manner (Fig. 6A). These results suggested that rivoceranib probably inhibited cyclin-D1 and downregulated VEGFR2 phosphorylation to reduce canine cell line viability in vivo.

Rivoceranib induces cell apoptosis and inhibits angiogenesis in vivo

Five tumour tissues per group that were selected randomly were sectioned and stained with TUNEL and anti-CD31 to evaluate the effects of rivoceranib on cell apoptosis and angiogenesis, respectively. We found

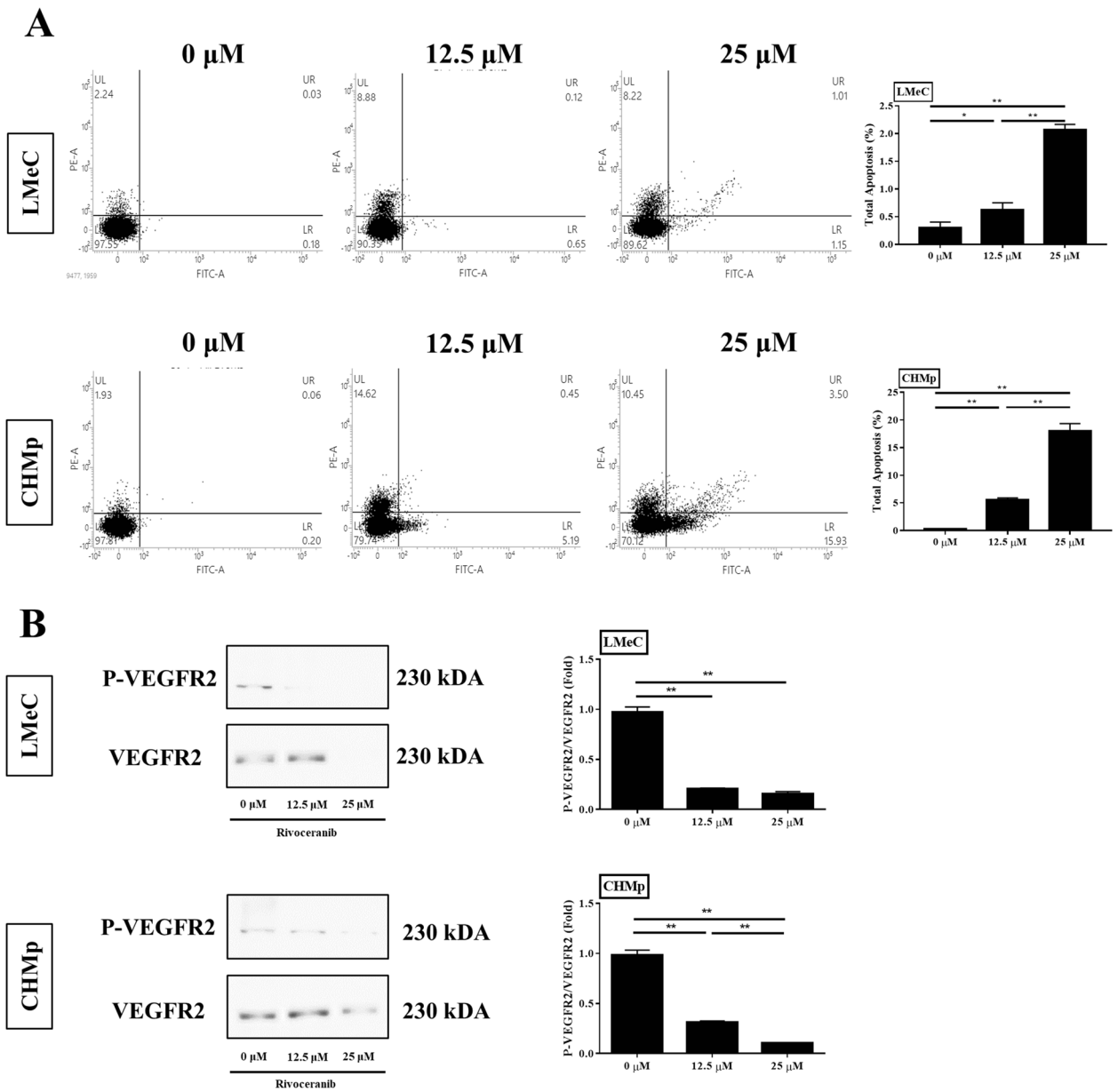

Fig. 3 Effects of rivoceranib on the migration of canine solid tumour cell lines in vitro. **A** Cell migration abilities of LMeC and CHMp were measured at 0, 12, and 24 h of rivoceranib treatment. **B** Histograms showing the relative gap size of the control group at 0 h after rivoceranib treatment. The data represent the mean ± standard deviation obtained from three independent experiments. * $p < 0.05$, ** $p < 0.01$

that rivoceranib treatment increased TUNEL-positive cells more than that observed with vehicle treatment in a dose-dependent manner in both cell lines (Fig. 6B). However, fewer CD31-positive cells were observed in the rivoceranib-treated tumour sections than in the control sections in both cell lines (Fig. 6C). Overall, these results indicated that rivoceranib showed apoptotic and anti-angiogenic activity in vivo.

Discussion

Rivoceranib is a highly selective VEGFR2 inhibitor and is a second-generation anti-angiogenic drug that has been approved for the treatment of solid tumours in humans [13, 21, 22]. Several studies have also shown that VEGFR2 is highly expressed in canine malignant tumours [23–27]. In addition, Prado et al. and Inteeworn et al. attempted to evaluate the anti-tumour effects of sorafenib, a VEGFR

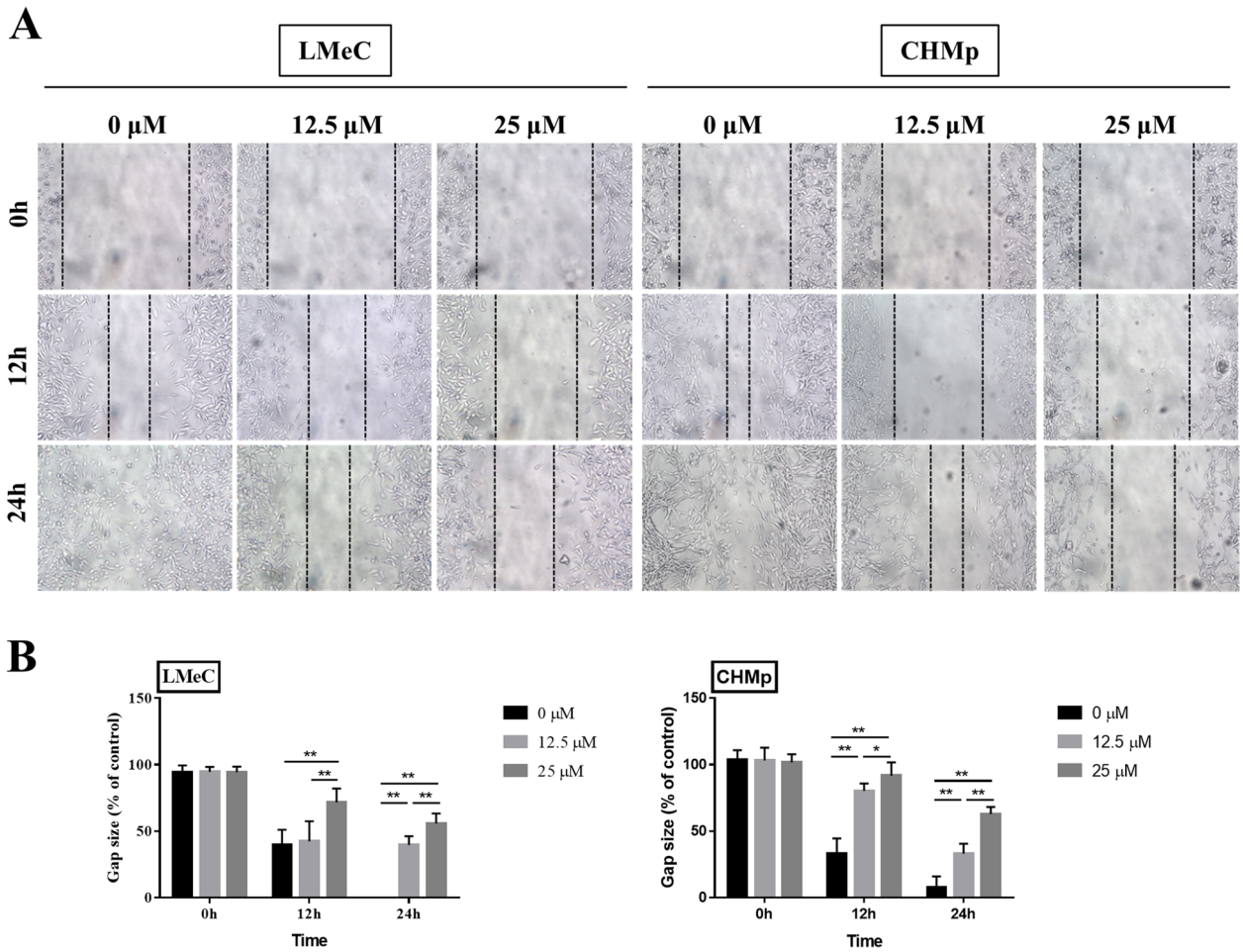

Fig. 4 Effects of rivoceranib on the apoptosis of canine solid tumour cell lines. The percentage of apoptotic cells was measured by flow cytometry. Total apoptotic cells were quantified using Annexin V (FITC) and propidium iodide (PI) dual staining. Annexin V^+/PI^- cells were considered to reflect early apoptosis, and Annexin V^+/PI^+ cells were considered to reflect late apoptosis. The data represent the mean ± standard deviation obtained from three independent experiments. * $p < 0.05$, ** $p < 0.01$

inhibitor, in canine tumour cells [28, 29]. In this study, we evaluated the anti-tumour effects of rivoceranib in mouse xenograft models of canine melanoma and MGT.

Recent studies have demonstrated that rivoceranib is effective against diverse types of human cell lines such as hepatocarcinoma, non-small cell lung cancer, melanoma, and breast cancer [30–33]. Consistent with the results of previous studies, our results indicate that the cytotoxic and anti-tumour effects of rivoceranib can be attributed to the enhancement of apoptosis, cell cycle arrest, and inhibition of migration in canine tumour cell lines in vitro. We also demonstrated that the expression levels of cyclin-D1 which are well known for playing a key role in tumour growth and proliferation [34, 35] were significantly reduced by rivoceranib treatment in a dose-dependent manner in both cell lines. Although rivoceranib showed anti-proliferative effects against canine tumour cell lines (LMeC and CHMp)

(See figure on next page.)

Fig. 5 In vivo effects of rivoceranib in the xenograft model. **A** The mean LMeC tumour volumes in the four groups (vehicle and 75 mg/kg, 150 mg/kg, and 300 mg/kg rivoceranib-treated; $n = 10$ in each group), and images of the collected tumours from the xenograft models after 29 days of treatment. **B** The mean CHMp tumour volumes in the four groups (vehicle and 75 mg/kg, 150 mg/kg, and 300 mg/kg rivoceranib-treated; $n = 10$ in each group), and images of the collected tumours from the xenograft models after 16 days of treatment. **C** The tumour weights and **D** body weights of mice were monitored twice a week during rivoceranib treatment in both cell lines. The data represent the mean ± standard deviation * $p < 0.05$, ** $p < 0.01$

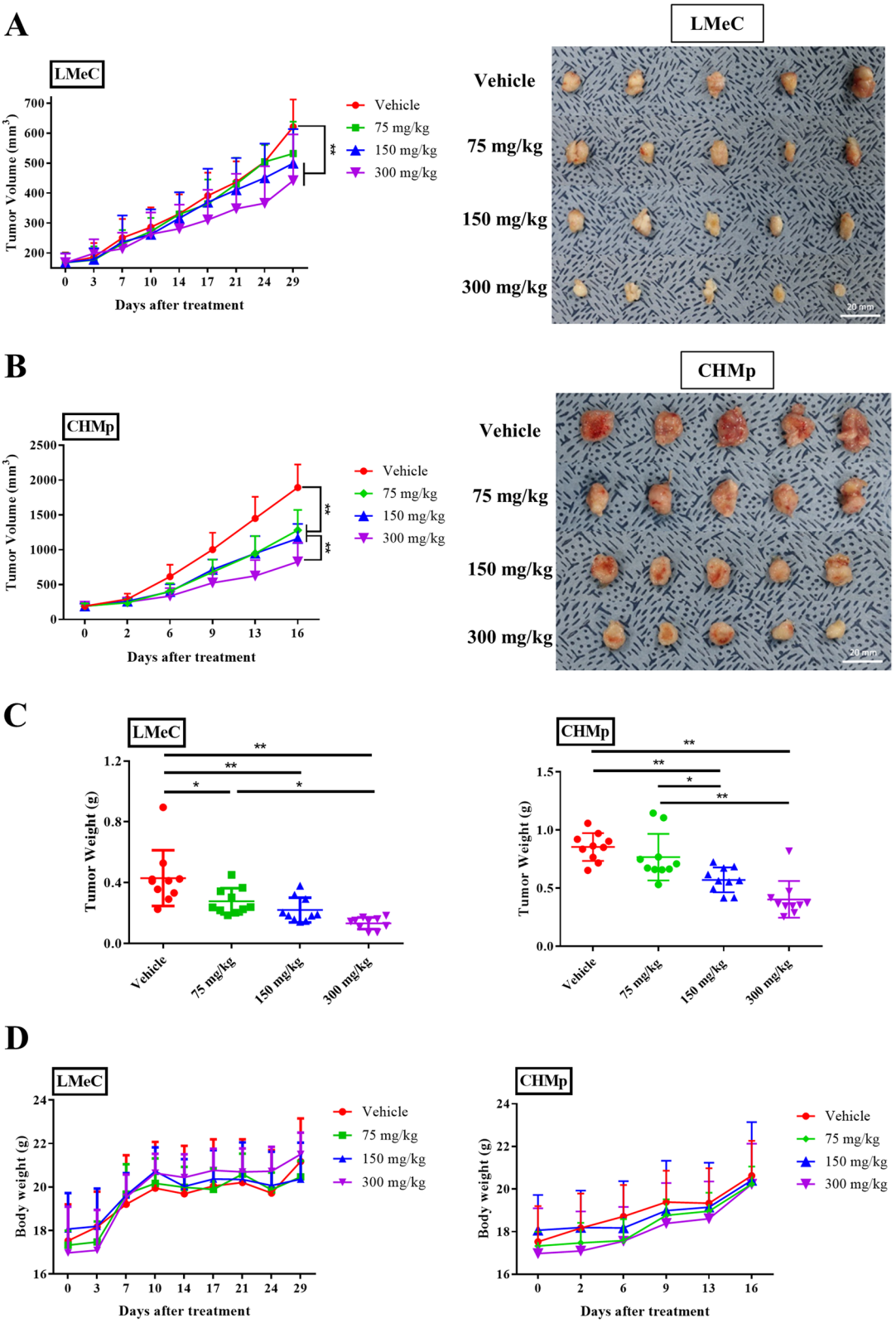

Fig. 5 (See legend on previous page.)

in vitro, it was difficult to evaluate whether these effects were associated with the VEGFR2 pathway because the canine tumour cell lines used in this study showed minimal expression of VEGFR2 in vitro (Supplementary Figure S1).

Therefore, we also determined the anti-tumour activity of rivoceranib in vivo with two xenograft mouse models of canine tumours: LMeC and CHMp. Interestingly, VEGFR2 was highly expressed in the tumours of xenograft mouse models containing LMeC and CHMp. After oral administration of rivoceranib at doses of 0, 75, 150, and 300 mg/kg in mice with LMeC or CHMp cells, the average tumour volume and weight were significantly reduced in a dose-dependent manner. Our western blot analysis results showed that rivoceranib significantly reduced the activity of VEGFR2 in vivo. Furthermore, evidence of the rivoceranib-induced increase in TUNEL-positive cells and fewer CD31-positive cells in treated tumour sections than in untreated tumour sections in both cell lines led us to hypothesise that rivoceranib reduced cell viability and tumour angiogenesis by inhibiting VEGF/VEGFR2 signalling.

The VEGFR family consists of VEGFR-1/Flt-1, VEGFR-2/KDR/Flk-1, and VEGFR-3/Flt-4 [33, 36, 37]. VEGFR2 exerts its biological function by coupling with VEGF cytokines to activate the VEGF/VEGFR2 signalling pathway, which is closely related to tumour angiogenesis and plays a crucial role in tumour cell adaptation to hostile environments [30, 38]. VEGF/VEGFR2 is well established to promote neighbouring vessel formation, thereby facilitating the delivery of nutrients for cancer cell survival, and previous reports have suggested that the expression of VEGFR2 correlates with poor prognosis [39, 40]. Rivoceranib is an oral anti-angiogenic drug that highly selectively inhibits VEGFR2 with a binding affinity 10 times higher than that of anti-angiogenic drugs sorafenib or vantalanib [14, 15].

There are some limitations in this study. First, we used a single cell line for canine melanoma and MGT. Second, as there are other anti-tumour underlying mechanisms, further studies using rivoceranib with other anti-tumour agents for synergic effects are needed. However, these results may provide a reference in veterinary medicine because this study was the first attempt to demonstrate the anti-tumour effects of rivoceranib in mouse xenograft models of canine tumours. Also, our data might provide scientific evidence for conducting clinical trials in canine patients.

Conclusions

Our results showed that rivoceranib inhibits proliferation, migration, and cell cycle progression in two canine tumour cell lines (LMeC for melanoma, and CHMp for MGT) in vitro. In addition, we showed that rivoceranib inhibits tumour growth in xenograft mouse models through the enhancement of apoptosis and anti-angiogenic effects by inhibiting the VEGFR2 pathway. These results suggest that rivoceranib, a selective VEGFR2 inhibitor, might be a novel anti-angiogenic therapy for dogs with melanoma or MGTs.

Methods

Cell culture

The canine MGT cell line (CHMp) and the canine melanoma cell line (LMeC) was kindly provided by Professor Nobuo Sasaki [19, 20]. LMeC and CHMp cells were incubated in Roswell Park Memorial Institute-1640 medium and supplemented with 10% foetal bovine serum (FBS) and 100 U/mL of penicillin/streptomycin at 37 °C in a humidified atmosphere with 5% CO_2. The medium was replaced every 2–3 days, and the cells were sub-cultured at 90% confluency.

Cell proliferation assay

Rivoceranib powder was provided by HLB Life Science Co., Ltd. (Gangnam-gu, Republic of Korea) and stored at room temperature (20–25 °C). To determine the concentration of rivoceranib that affects canine cell line viability and proliferation, a cell proliferation assay was performed as described previously [18]. Briefly, a density of 1×10^3 cells were plated onto 96-well cell culture plates (SPL Life Science, Pocheon, Korea) with 100 μL of culture medium containing rivoceranib (0, 3.125, 6.25, 12.5, 25, 50, or 100 μM). After culturing for 24, 48, and 72 h, the cell number was determined using the D-plus^{tm} CCK-8 assay (Dong-in Biotech, Seoul, Korea) according to the manufacturer's instructions. Wells containing culture medium or 0.5% dimethyl sulfoxide with culture medium were used as the control group.

(See figure on next page.)

Fig. 6 Effects of rivoceranib on tumour tissue in vivo. **A** The collected tumour tissues were subjected to western blot analysis for the evaluation of VEGFR2 activity and the expression levels of cyclin-D1. The intensity of the bands on the films was evaluated as the relative ratio of phosphorylated-VEGFR2 (P-VEGFR2) to the band intensity of VEGFR2 and the ratio of cyclin-D1 to the band intensity of β-actin. Cropped bands are displayed. Samples were derived from same experiment, and blots were processed in parallel. **B**, **C** TUNEL and anti-CD31 staining images of tumour sections in each group (vehicle and 75 mg/kg, 150 mg/kg, and 300 mg/kg rivoceranib-treated). TUNEL- and CD31-positive cells were counted in five random fields per group under a microscope. The data represent the mean ± standard deviation. * $p < 0.05$, ** $p < 0.01$ versus control group (vehicle group)

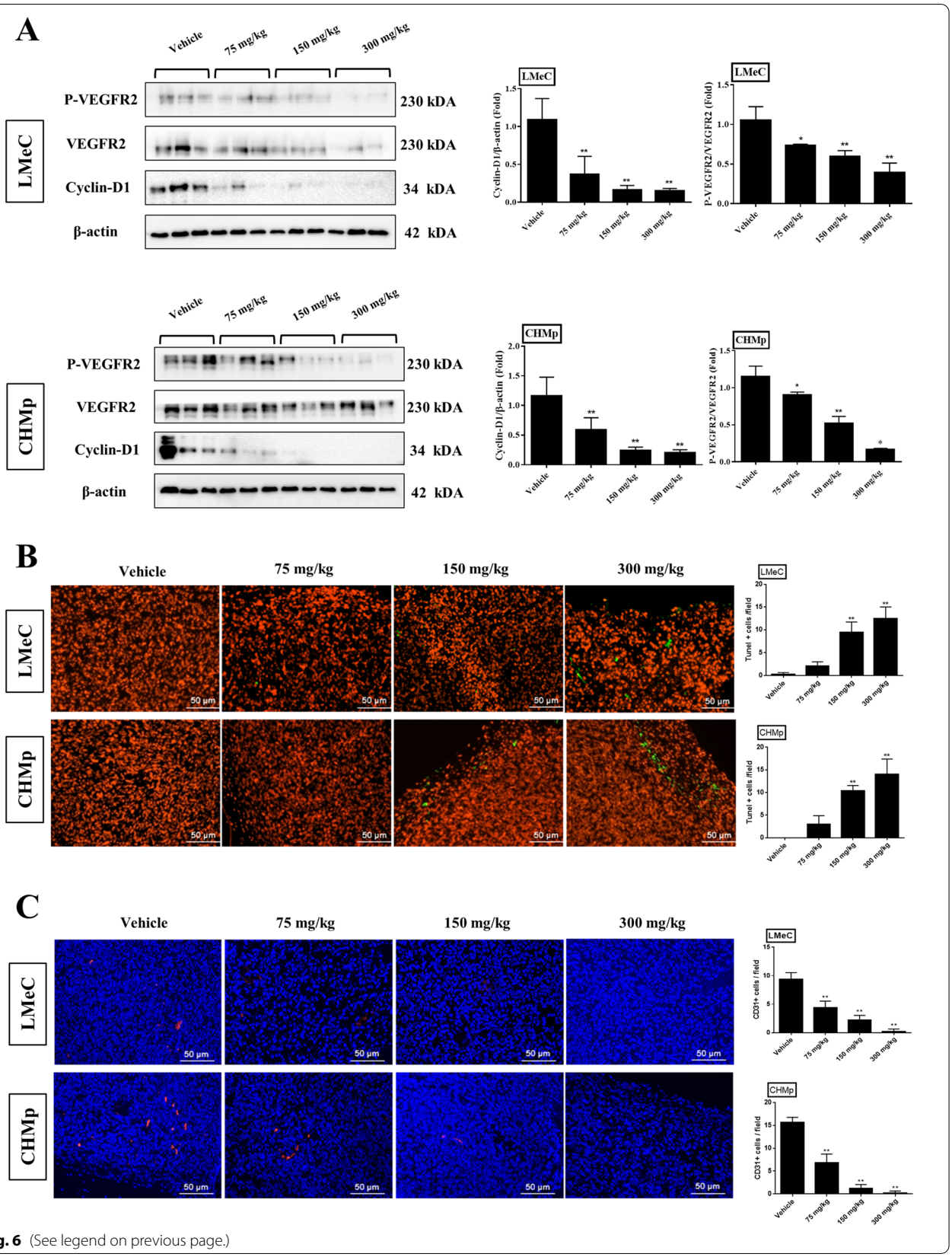

Fig. 6 (See legend on previous page.)

Cell cycle assay

For cell cycle assay, as described previously [41], LMeC and CHMp cells were cultured in 6-well cell culture plates, allowed to adhere, and further cultured with increasing concentrations of rivoceranib (0, 12.5, and 25 μM). After 48 h, 1×10^5 cells were collected, washed with cold PBS, and fixed with 70% cold alcohol at -20 °C for 2 h. The cells were then collected, washed again with PBS, and incubated with 500 μL of PI/RNase buffer (BD Biosciences, San Diego, CA, USA) for 30 min at room temperature. The samples were analysed using flow cytometry FACS (AriaII flow cytometer; BD Bioscience, San Jose, CA, USA).

Wound-healing assay

The migration abilities of the cell lines were determined using a wound-healing assay as described previously [18]. Briefly, the cells were seeded in a 12-well culture plate at a density of 1×10^5 cells/well. After reaching 100% confluence, the cells were induced using 2 μg/mL of mitomycin (EnzoLife Science, Farmingdale, NY, USA) for 2 h. The cells were manually scratched using a sterile 1000-μL pipette tip, and suspended cells were removed using phosphate-buffered saline (PBS). The various groups of adherent cells were cultured in serum-reduced complete medium (2% FBS) with rivoceranib (0, 12.5, and 25 μM). Cell migration was observed and captured under a microscope using the T Capture program (Tucsen Photonics, Fuzhou, China) at 0, 12, and 24 h. The migration ability was calculated relative to the gap size of the control group at 0 h.

Apoptosis analysis

LMeC and CHMp cells were seeded in 6-well cell culture plates at a density of 1×10^5 cells, allowed to adhere, and treated with different concentrations of rivoceranib (0, 12.5, and 25 μM) for 48 h. The cells were then dual-stained with annexin V and PI using the Annexin V Apoptosis Detection Kit I (BD Pharmingen, San Diego, CA, USA) as described previously [18]. The apoptosis rate of CHMp cells was analysed using a FACS cytometer (BD Bioscience, San Diego, CA, USA).

Mouse xenograft model

Female NOD.CB17-Prkdc^{SCID}/Acr mice aged 6 weeks and weighing 18–22 g were purchased from Raon Bio (Yongin, Korea). All mice were housed in a specific pathogen-free standard room under controlled temperature (19–23 °C) and humidity (50 ± 20%) conditions and a 12-h light–dark cycle. The study and all experimental procedures involving animals were approved by the Institutional Animal Care and Use Committee of KPC (P194007), and the experiments were performed in compliance with the guidelines for animal experiments. The study was also carried out in compliance with the ARRIVE guidelines. To induce tumours in the mice, 5×10^6 CHMp cells or 1×10^7 LMeC cells were suspended in 100 μL of PBS, mixed with 100 μL of Corning® Matrigel® Matrix (1:1 dilution, Corning Inc., New York, NY, USA), and then injected subcutaneously into the right flank of each mouse, as described previously [5]. After the predetermined inoculation and treatment periods, tumour dimensions were measured, and the volume was calculated using the following formula: $0.5 \times \text{width}^2 \times \text{length}$. The weight and tumour volume of the mice were monitored every 3–4 days. Mice were sacrificed on day 16 for the canine melanoma model and day 29 for the canine MGT model. Tissue samples of tumour were collected for further processing.

Rivoceranib treatment

For rivoceranib administration, the reagent powder was dissolved in 0.5% carboxymethylcellulose (CMC; Sigma-Aldrich, St. Louis, MO, USA) solution. As described previously [42], when the tumours reached an average volume of 150–200 mm^3, the mice were randomised into the following four groups ($n = 10$ each) and were orally treated as indicated: Group 1, 10 mL/kg 0.5% CMC solution (vehicle); and Groups 2, 3, and 4 were administered 75, 150, and 300 mg/kg rivoceranib, respectively, in 10 mL/kg of the vehicle. Rivoceranib and the vehicle were administered daily for 15 (CHMp) or 28 (LMeC) consecutive days, after which all mice were euthanized and tumour tissue samples were collected for further analysis.

Western blot analysis

Total protein from the collected cell lines and tissue was extracted in PRO-PREP Protein Extraction Solution (Intron Biotechnology, Seongnam, Korea) on ice according to the manufacturer's instructions. The protein concentration was measured using the Bio-Rad DC Protein Assay Kit (Bio-Rad, Hercules, CA, USA) as described previously [43]. The collected proteins (30 μg) were separated using sodium dodecyl sulphate gel electrophoresis, and the protein bands were transferred onto polyvinylidene difluoride membranes (EMD Millipore, Billerica, MA, USA). The membranes were incubated in 5% non-fat dry milk in Tris-buffered saline containing 0.1% Tween 20 for 1 h and incubated with antibodies against anti-cyclin-D1 (1:1000; LSBio, Seattle, WA, USA) and anti-phospho-VEGFR2 (1:1000; Cell Signaling Technology, Beverly, MA, USA) at 4 °C overnight. The membranes were incubated with anti-mouse or anti-rabbit immunoglobulin G (Santa Cruz Biotechnology, Dallas, Texas, USA) as the secondary antibodies (1:2000) for 1 h. Immunoreactive bands were normalised to β-actin (1:1000; Santa Cruz) or VEGFR2 (1:1000; Cell Signaling Technology) and visualised using SuperSignal

West Pico PLUS Chemiluminescent substrate (Advansta, Menlo Park, CA, USA).

Immunofluorescence analysis

Xenograft tumour tissues obtained from mice were fixed in 10% formalin, and paraffin-embedded 4-μm-thick tissue sections were deparaffinised in xylene and rehydrated with ethanol. The tumour apoptosis rates were determined based on TUNEL staining (Apo-BrdU DNA Fragmentation Assay Kit; BioVision, San Francisco, USA), as described previously [5]. For the analysis of angiogenesis ability in the tumour tissue, the slides were incubated overnight at 4 °C with antibodies against CD31 (1:100; Thermo Fisher Scientific, Waltham, MA, USA). After washing three times, the tumour sections were incubated with the secondary antibody (1:200; sc-516251; Santa Cruz Biotechnology) for 1 h at room temperature (protected from light). Finally, the slides were mounted in Vectashield mounting medium containing 4,6-diamidino-2-phenylindole (Vector Laboratories, Burlingame, CA, USA). The immunoreactive cells were counted in six random fields per group using an EVOS FL microscope (Life Technologies, Darmstadt, Germany).

Statistical analysis

Data are shown as mean ± standard error. Differences between the groups were compared by one-way analysis of variance or Student's t-test using GraphPad Prism v.6.01 software (GraphPad Inc., La Jolla, CA, USA). A value of $P < 0.05$ was considered statistically significant.

Abbreviations

MGT: Mammary gland tumour; VEGF: Vascular endothelial growth factor; VEGFRs: Vascular endothelial growth factor receptors; FACS: Fluorescence-activated cell sorting; FBS: Foetal bovine serum; CCK: Cell counting kit; PBS: Phosphate-buffered saline.

Supplementary Information

The online version contains supplementary material available at https://doi.org/10.1186/s12917-021-03026-1.

Additional file 1: Supplementary Figure S1. Western blot analysis of total and phosphorylated VEGFR2 in tumour cell lines (LMec and CHMp). The expression levels of total and phosphorylated VEGFR2 are weak for in vitro experiments. Cropped bands are displayed. Samples were derived from same experiment, and blots were processed in parallel.

Additional file 2: Supplementary Figure S2. The full-length blots with specific protein bands used in this study. (A) The full-length blots used in Fig. 1B. (B,C) The full-length blots used in Fig. 6A.

Acknowledgements

The authors would like to express gratitude to the Research Institute for Veterinary Science at the College of Veterinary Medicine, Seoul National University.

Authors' contributions

QL and YSK contributed to the conception and design, collection and/or assembly of data, data analysis and interpretation, and manuscript writing. JHA contributed to the conception and design, collection and/or assembly of data, and manuscript writing. JAK and SHH contributed to the provision of study material or patients, collection and/or assembly of data. WJS and HYY contributed to conception and design, data analysis and interpretation, manuscript writing and final approval of the manuscript. All authors have read and approved the final manuscript.

Funding

This research was supported by Basic Science Research Program to Research Institute for Basic Sciences (RIBS) of Jeju National University through the National Research Foundation of Korea (NRF) funded by the Ministry of Education (2019R1A6A1A10072987).

Availability of data and materials

The data that support the findings of this study are available from the corresponding author upon reasonable request.

Declarations

Ethics approval and consent to participate

The experimental protocol was established according to the ethical guidelines of the Helsinki Declaration and was approved by the Institutional Animal Care and Use Committee of KPC (P194007). The experiments were also carried out in compliance with the ARRIVE guidelines.

Consent for publication

Not applicable.

Competing interests

None of the authors have a financial or personal relationship with people or organisations that could inappropriately influence or bias the content of the paper.

Author details

[1]Department of Veterinary Medicine, College of Agriculture, YanBian University, YanJi, JiLin, China. [2]Laboratory of Veterinary Internal Medicine, Department of Veterinary Clinical Science, College of Veterinary Medicine, Seoul National University, Seoul 08826, Republic of Korea. [3]KPC Corporation, Oporo, Opo-eup, Gwangju-si, Gyeonggi-do, Korea. [4]HLB LifeScience Co., Ltd., Teheran-ro, Gangnam-gu, Seoul, Republic of Korea. [5]Department of Veterinary Internal Medicine and Research Institute of Veterinary Science, College of Veterinary Medicine, Jeju National University, Jeju 63243, Republic of Korea.

Received: 18 January 2021 Accepted: 7 September 2021
Published online: 26 October 2021

References

1. London CA, Hannah AL, Zadovoskaya R, Chien MB, Kollias-Baker C, Rosenberg M, Downing S, Post G, Boucher J, Shenoy N, Mendel DB, McMahon G, Cherrington JM. Phase I dose-escalating study of SU11654, a small molecule receptor tyrosine kinase inhibitor, in dogs with spontaneous malignancies. Clin Cancer Res. 2003;9(7):2755–68.
2. Goldschmidt MH. Pigmented lesions of the skin. Clin Dermatol. 1994;12(4):507–14.
3. Smith SH, Goldschmidt MH, McManus PM. A comparative review of melanocytic neoplasm. Vet Pathol. 2002;39(6):651–78.
4. Rutteman GR, Erich SA, Mol JA, Spee B, Grinwis GCM, Fleckenstein L, London CA, Efferth T. Safety and efficacy field study of artesunate for dogs with non-resectable tumours. Anticancer Res. 2013;33(5):1819–27.
5. Tran CM, Moore AS, Frimberger AE. Surgical treatment of mammary carcinomas in dogs with or without postoperative chemotherapy. Vet Comp Oncol. 2014;14(3):252–62.
6. Brockley LK, Cooper MA, Bennett PF. Malignant melanoma in 63 dogs (2001–2011): the effect of carboplatin chemotherapy on survival. New Zeal Vet J. 2013;61(1):25–31.
7. Rossi F, Sabattini S, Vascellari M, Marconato L. The impact of toceranib, piroxicam and thalidomide with or without hypofractionated radiation therapy on clinical outcome in dogs with inflammatory mammary carcinoma. Vet Comp Oncol. 2018;16(4):497–504.

8. Hanahan D, Weinberg RA. The hallmarks of cancer. Cell. 2000;100(1):57–70.
9. Hanahan D, Weinberg RA. Hallmarks of cancer: the next generation. Cell. 2011;144(5):646–74.
10. Kerbel RS. Antiangiogenic therapy: a universal chemosensitization strategy for cancer? Science. 2006;312(5777):1171–5.
11. Zhang Z, Zhao Y, Lu F, Hou X, Ma Y, Luo F, Zeng K, Zhao S, Zhang Y, Zhou T, Yang Y, Fang W, Huang Y, Zhang L, Zhao H. Multi-targeted tyrosine kinase inhibitors as third-line regimen in advanced non-small cell lung cancer: a nerk meta-analysis. Ann Transl Med. 2019;7(18):452.
12. Roviello G, Petrioli R, Marano L, Polom K, Marrelli D, Perrella A, Roviello F. Angiogenesis inhibitors in gastric and gastroesophageal junction cancer. Gastric Cancer. 2016;19(1):31–41.
13. Scott LJ. Apatinib: a review in advanced gastric cancer and other advanced cancers. Drugs. 2018;78(7):747–58.
14. Yu GC, Yang J, Ye B, Xu LL, Li XY, Zheng GR. Apatinib in the treatment of advanced non-small-cell lung cancer: a meta-analysis. Math Biosci Eng. 2019;16(6):7659–70.
15. Hu X, Cao J, Hu W, Wu C, Pan Y, Cai L, Tong Z, Wang S, Li J, Wang Z, Wang B, Chen X, Yu H. Multicenter phase II study of apatinib in non-triple-negative metastatic breast cancer. BMC Cancer. 2014;14(1):820.
16. Langer CJ, Mok T, Postmus PE. Targeted agents in the third-/fourth-line treatment of patients with advanced (stage III/IV) non-small cell lung cancer (NSCLC). Cancer Treat Rev. 2013;39(3):252–60.
17. Li J, Qin S, Xu J, Guo W, Xiong J, Bai Y, Sun G, Yang Y, Wang L, Xu N, Cheng Y, Wang Z, Zheng L, Tao M, Zhu X, Ji D, Liu X, Yu H. Apatinib for chemotherapy-refractory advanced metastatic gastric cancer: results from a randomized, placebo-controlled, parallel-arm, phase II trial. J Clin Oncol. 2013;31(26):3219–25.
18. Lee JH, Li Q, An JH, Chae HK, Choi JW, Kim BJ, Song WJ, Youn HY. Antitumor activity of rivoceranib against canine mammary gland tumor cell lines. Anticancer Res. 2019;39:5483–94.
19. Uyama R, Nakagawa T, Hong SH, Mochizuki M, Nishimura R, Sasaki N. Establishment of four pairs of canine mammary tumour cell lines derived from primary and metastatic origin and their E-cadherin expression. Vet Comp Oncol. 2006;4(2):104–13.
20. Inoue K, Ohashi E, Kadosawa T, Hong SH, Matsunaga S, Mochizuki M, Nishimura R, Sasaki N. Establishment and characterization of four canine melanoma cell lines. J Vet Med Sci. 2004;66(11):1437–40.
21. Scott A, Messersmith W, Jimeno A. Apatinib: a promising oral antiangiogenic agent in the treatment of multiple solid tumors. Drugs Today (Barcelona, Spain: 1998). 2015;51(4):223–9.
22. Ding J, Chen X, Gao Z, Dai X, Li L, Xie C, Jiang H, Zhang L, Zhong D. Metabolism and pharmacokinetics of novel selective vascular endothelial growth factor receptor-2 inhibitor apatinib in humans. Drug Metab Dispos. 2013;41(6):1195–210.
23. Santos A, Lopes C, Gärtner F, Matos A. VEGFR-2 expression in malignant tumours of the canine mammary gland: a prospective survival study. Vet Comp Oncol. 2016;14(3):e83–92.
24. Kimura M, Yamasaki M, Satoh H, Uchida N. Repeatable and objective method for evaluating angiogenesis using real-time RT-PCR of endoglin expression in canine tumours. Vet Comp Oncol. 2021;19(1):34–43.
25. Brocca G, Ferraresso S, Zamboni C, Martinez-Merlo EM, Ferro S, Goldschmidt MH, Castagnaro M. Array comparative genomic hybridization analysis reveals significantly enriched pathways in canine oral melanoma. Front Oncol. 2019;9:1397.
26. Thompson JJ, Morrison JA, Pearl DL, Boston SE, Wood GA, Foster RA, Coomber BL. Receptor tyrosine kinase expression profiles in canine cutaneous and subcutaneous mast cell tumors. Vet Pathol. 2016;53(3):545–58.
27. Shiomitsu K, Johnson CL, Malarkey DE, Pruitt AF, Thrall DE. Expression of epidermal growth factor receptor and vascular endothelial growth factor in malignant canine epithelial nasal tumours. Vet Comp Oncol. 2009;7(2):106–14.
28. Prado M, Macedo S, Guiraldelli G, Lainetti PF, Leis-Filho AF, Kobayashi PE, Laufer-Amorim R, Fonseca-Alves CE. Investigation of the prognostic significance of vasculogenic mimicry and its inhibition by sorafenib in canine mammary gland tumors. Front Oncol. 2019;9:1445.
29. Inteeworn N, Ohlerth S, Hopfl G, Guscetti F, Bley CR, Wergin MC, Roos M, Gassmann M, Kaser-Hotz B. Simultaneous application of the vascular endothelial growth factor (VEGF) receptor inhibitor PTK787/ZK 222584 and ionizing radiation does not further reduce the growth of canine oral melanoma xenografts in nude mice. Vet J. 2007;3:564–70.
30. Gao Z, Shi M, Wang Y, Chen J, Ou Y. Apatinib enhanced anti-tumor activity of cisplatin on triple-negative breast cancer through inhibition of VEGFR-2. Pathol Res Pract. 2019;215(7):152422.
31. Liao J, Jin H, Li S, Xu L, Peng Z, Wei G, Long J, Guo Y, Kuang M, Zou Q, Peng S. Apatinib potentiates irradiation effect via suppressing PI3K/AKT signaling pathway in hepatocellular carcinoma. J Exp Clin Cancer Res. 2019;38(1):1–13.
32. Zhang Q, Song Y, Cheng X, Xu Z, Mattew OA, Wang J, Sun Z, Zhang X. Apatinib reverses paclitaxel-resistant lung cancer cells (A549) through blocking the function of ABCB1 transporter. Anticancer Res. 2019;39(10):5461–71.
33. Liu Z, Zhou YJ, Ding RL, Xie F, Fu SZ, Wu JB, Ynag LL, Wen QL. In vitro and in vivo apatinib inhibits vasculogenic mimicry in melanoma MUM-2B cells. PLoS ONE. 2018;13(7):e0200845.
34. Tashiro E, Tsuchiya A, Imoto M. Functions of cyclin D1 as an oncogene and regulation of cyclin D1 expression. Cancer Sci. 2007;98(5):629–35.
35. Alao JP. The regulation of cyclin D1 degradation: roles in cancer development and the potential for therapeutic invention. Mol Cancer. 2007;6:24.
36. Qin S. Phase III study of apatinib in advanced gastric cancer: a randomized, double-blind, placebo-controlled trial. Ann Oncol. 2014;25(2):ii117.
37. Zhang Y, Han C, Li J, Zhang L, Wang L, Ye S, Hu Y, Bai L. Efficacy and safety for Apatinib treatment in advanced gastric cancer: a real world study. Sci Rep. 2017;7(1):1–9.
38. Nishida N, Yano H, Nishida T, Kamura T, Kojiro M. Angiogenesis in cancer. Vasc Health Risk Manag. 2006;2(3):213.
39. Peng H, Zhang Q, Li J, Zhang N, Hua Y, Xu L, Deng Y, Lai J, Peng Z, Peng B, Chen M, Peng S, Kuang M. Apatinib inhibits VEGF signaling and promotes apoptosis in intrahepatic cholangiocarcinoma. Oncotarget. 2016;7(13):17220.
40. Lian L, Li XL, Xu MD, Li XM, Wu MY, Zhang Y, Tao M, Li W, Shen XM, Zhou C, Jiang M. VEGFR2 promotes tumorigenesis and metastasis in a pro-angiogenic-independent way in gastric cancer. BMC Cancer. 2019;19(1):183.
41. Kweon K, Ahn JO, Song WJ, Li Q, Lee BY, Chae HK, Youn HY. Antitumor effects of SB injection in canine osteosarcoma and melanoma cell lines. In Vitro Cell Dev-An. 2019;55(1):7–16.
42. Tian S, Quan H, Xie C, Guo H, Lu F, Xu Y, Li J, Lou L. YN968D1 is a novel and selective inhibitor of vascular endothelial growth factor receptor-2 tyrosine kinase with potent activity in vitro and in vivo. Cancer Sci. 2011;102(7):1374–80.
43. Yang JI, Jin B, Kim SY, Li Q, Nam A, Ryu MO, Lee WW, Son MH, Park HJ, Song WJ, Youn HY. Antitumour effects of Liporaxel (oral paclitaxel) for canine melanoma in a mouse xenograft model. Vet Comp Oncol. 2020;18(2):152–60.

Publisher's Note